Video Article

Utilization of Ultrasound Guided Tissue-directed Cellular Implantation for the Establishment of Biologically Relevant Metastatic Tumor Xenografts

Tina T. Thomas[1], Sahiti Chukkapalli[1], Raelene A. Van Noord[1], Melanie Krook[2], Mark J. Hoenerhoff[3], Jonathan R. Dillman[4], Elizabeth R. Lawlor[2,5], Valerie P. Opipari[5], Erika A. Newman[1]

[1]Departments of Surgery, C.S Mott Children's and Women's Hospital, The University of Michigan Medical School

[2]Departments of Pathology, C.S Mott Children's and Women's Hospital, The University of Michigan Medical School

[3]Unit for Laboratory Animal Medicine, The University of Michigan Medical School

[4]Departments of Radiology, C.S Mott Children's and Women's Hospital, The University of Michigan Medical School

[5]Departments of Pediatrics, C.S Mott Children's and Women's Hospital, The University of Michigan Medical School

Correspondence to: Erika A. Newman at eanewman@med.umich.edu

URL: https://www.jove.com/video/57558
DOI: doi:10.3791/57558

Keywords: Retraction, Issue 135, Ewing's sarcoma, neuroblastoma, orthotopic, preclinical model, ultrasound, xenograft

Date Published: 5/25/2018

Citation: Thomas, T.T., Chukkapalli, S., Van Noord, R.A., Krook, M., Hoenerhoff, M.J., Dillman, J.R., Lawlor, E.R., Opipari, V.P., Newman, E.A. Utilization of Ultrasound Guided Tissue-directed Cellular Implantation for the Establishment of Biologically Relevant Metastatic Tumor Xenografts. *J. Vis. Exp.* (135), e57558, doi:10.3791/57558 (2018).

Abstract

Preclinical testing of anticancer therapies relies on relevant xenograft models that mimic the innate tendencies of cancer. Advantages of standard subcutaneous flank models include procedural ease and the ability to monitor tumor progression and response without invasive imaging. Such models are often inconsistent in translational clinical trials and have limited biologically relevant characteristics with low proclivity to produce metastasis, as there is a lack of a native microenvironment. In comparison, orthotopic xenograft models at native tumor sites have been shown to mimic the tumor microenvironment and replicate important disease characteristics such as distant metastatic spread. These models often require tedious surgical procedures with prolonged anesthetic time and recovery periods. To address this, cancer researchers have recently utilized ultrasound-guided injection techniques to establish cancer xenograft models for preclinical experiments, which allows for rapid and reliable establishment of tissue-directed murine models. Ultrasound visualization also provides a noninvasive method for longitudinal assessment of tumor engraftment and growth. Here, we describe the method for ultrasound-guided injection of cancer cells, utilizing the adrenal gland for NB and renal sub capsule for ES. This minimally invasive approach overcomes tedious open surgery implantation of cancer cells in tissue-specific locations for growth and metastasis, and abates morbid recovery periods. We describe the utilization of both established cell lines and patient derived cell lines for orthotopic injection. Pre-made commercial kits are available for tumor dissociation and luciferase tagging of cells. Injection of cell suspension using image-guidance provides a minimally invasive and reproducible platform for the creation of preclinical models. This method is utilized to create reliable preclinical models for other cancers such as bladder, liver and pancreas exemplifying its untapped potential for numerous cancer models.

Video Link

The video component of this article can be found at https://www.jove.com/video/57558/

Introduction

Animal xenograft models are essential tools for preclinical studies of novel anticancer therapies. Standard murine xenografts rely on subcutaneous flank implantation of cells, providing an efficient and easily accessible site for monitoring tumor growth. The disadvantage of subcutaneous models is their lack of tumor-specific biologic characteristics, which may limit their potential to metastasize[1]. Such limitations are overcome by the use of orthotopic xenografts in which tumor cells are engrafted at native tissue sites, providing a relevant microenvironment with metastatic potential[2]. Orthotopic xenograft models maintain original biological features and provide reliable models for preclinical drug discovery[3,4]. The cancer cells utilized for tissue-directed implantation are either established cell lines or patient-derived cells from patient tumors. Xenografts established from cancer cell lines may exhibit high genetic divergence from the primary tumor compared to patient derived xenografts[5]. Given this, the establishment of patient-derived orthotopic xenografts has become the preferred standard for testing novel therapeutics in cancer drug discovery.

In the pediatric cancer neuroblastoma (NB), orthotopic xenograft models recapitulate primary tumor biology and develop metastasis to typical sites of NB spread[6,7]. NB develops in the adrenal gland or along the paravertebral sympathetic chain. The most common methods of orthotopic implantation require open trans-abdominal surgical procedures. Such methods are often tedious, have high animal morbidity, and complex recovery periods. High-resolution ultrasound has been recently utilized for tissue-directed implantation of tumor cells in development of several murine models for cancer research[8,9]. The technique is reliable, reproducible, efficient, and safe for the establishment of relevant metastatic tumor xenografts[10,11].

The establishment of pediatric cancer xenografts by ultrasound-guided target organ localization and needle implantation of cell lines and patient-derived tumor cells is demonstrated[11]. The technique was utilized for NB targeted to the murine adrenal gland. Ewing's sarcoma (ES) is predominantly an osseous cancer, commonly seen in the long bones such as femur and pelvic bones[12]. Case reports have shown that to determine whether growth of a predominantly osseous cancer is feasible in renal tissue, a renal sub capsular location was chosen for orthotopic implantation[13]. Renal sub capsular cell implantation of tumor cells has been utilized as a promising model to study spontaneous metastases for ES[14].

Protocol

All work was done in accordance with The University of Michigan Institutional Review Board (HUM 00052430) and conforms to procedures approved by the University Committee on Use and Care of Animals (UCUCA). The Unit for Laboratory of Animal Medicine (ULAM) oversaw animal care.

All work was done with approval from The University of Michigan Institutional Review Board (HUM 00052430) and conforms to all human research ethics committee regulations. Human cells are considered to be a potentially biohazardous material, so follow all special precautions and appropriate biosafety practices that are required by your institution. NSG mice are severely immunocompromised and susceptible to disease caused by bacteria commonly found in the environment.
Always use strict sterile technique when preparing materials for implantation and performing the injections.

1. Cell Culture

1. Grow established human NB cell lines (SH-SY5Y, SK-N-BE2, and IMR32) in minimal essential medium, supplemented with 10% fetal bovine serum, 2 mM glutamine, 100 units/mL penicillin, and 100 µg/mL streptomycin. Supplement IMR32 cells further with 1 mM pyruvate and 0.075% $NaHCO_3$. Maintain all cells at 37 °C, 5% CO_2 and 70-80% confluence.
2. Grow human ES cell lines (TC32, A673, CHLA-25, and A4573) in RPMI medium supplemented with 10% fetal bovine serum and 6 mM L-glutamine. Maintain all cells at 37 °C, 5% CO_2 at 70-80% confluence.
3. Send all cell lines for authentication.
   NOTE: Cell authentication is done at an outside facility, please refer to acknowledgements.

2. Preparation of Primary Patient-Derived Tumor Cells

1. With patient consent and assent, harvest discarded human NB tumor tissue from patients undergoing surgical resection for local control and transport to the laboratory in tissue storage solution for preservation.
   NOTE: All patient samples are de-identified and handled in accordance with Institutional Review Board guidelines.
2. Generate a single patient-derived cancer cell suspension (UMNBL001, UMNBL002) from tumor tissue using a tumor dissociation kit. Transfer approximately 0.5 g of tumor to a 100 mm cell culture dish containing 5 mL of RPMI buffer, 200 µL of enzyme H, 100 µL of enzyme R and 25 µL of enzyme A from the human tumor dissociation kit.
3. Mince the tumor into small pieces (2-4 mm each) using scissors and tissue forceps. Mix these fragments with the solutions in step 2.2.
4. Pipette the tumor mixture into a dissociator tube and close the tube. Invert the tube and attach onto the sleeve of the tissue dissociator. Run on program h_tumor_01.
5. Incubate the tumor cell suspension obtained above at 37 °C for 1 h on a rotating rack with intermittent trituration every 15 min.
6. Transfer the cell suspension to a new 50 mL conical tube and add 10 mL of RPMI. Centrifuge the cell suspension at 314 x g for 5 min.
7. Remove the supernatant and suspend the pellet in 5 mL of RPMI. Pass this solution through a 40 µm cell strainer and collect the strained solution into a fresh 50 mL conical tube. Wash this strainer once with 5 mL of RPMI media and centrifuge the mixture at 314 x g for 5 min to collect a pellet.
8. Measure the cell density using a hemacytometer[15]. Suspend the pellet obtained from above in RPMI to obtain a final concentration of 4×10^5 cells/10 µL. Take 5 µL of this cell suspension and 5 µL of matrigel to make 10 µL of cell solution for each injection.
   NOTE: Amount of RPMI used depends on the cell density measurement. For example, if the measured cell density of the obtained pellet is 4×10^5 cells, suspend the pellet in 10 µL of RPMI.

3. Luciferase Tagging of Cancer Cells

1. Make 10 mL of transduction media with 5 mL of viral supernatant EF1a-Luc2-IRES-mCherry and 5 mL of stem cell media. Add 7.5 µL of 1x polybrene.
2. Mix 5×10^6 cancer cells in transduction media and plate in 100 mm ultra-low attachment plate. Incubate at 37 °C and 5% CO_2 overnight.
   NOTE: As low attachment plates are used, cells will not adhere to plate.
3. After 24 h, bring the 100 mm plate containing cells under tissue culture hood and transfer the mixture into a 15 mL conical tube. Centrifuge the cell suspension at 314 x g for 5 min to get the cell pellet. Wash the cell pellet once with 1 mL of 1x phosphate-buffered saline (PBS) and suspend the cell pellet in 1 mL of HBSS containing 1% fetal bovine serum (FBS).
   1. Sort luciferase cells based on GFP-positive signal on fluorescence-activated cell sorting (FACS) analysis. Plate the sorted cells on 100 mm tissue culture treated dish and maintain at 70-80% confluence, 37 °C and 5% CO_2 until required.
4. Confirm luciferase signal with luciferase assay kit. Plate 10×10^4 sorted cells per well in an illuminometer compatible 96 well plate and incubate cells overnight at 37 °C and 5% CO_2. After 24 h, bring the 96 well plate to room temperature and add Steady-Glo reagent to cultured media in wells in 1:1 ratio. Allow cells to lyse for 5 min and read luminescence in spectrophotometer.
5. Bring the 100 mm dish under a tissue culture hood. Discard the supernatant media. Wash the cells once with 2 mL of 1x PBS.

6. Add 2 mL of 0.25% trypsin and return the 100 mm dish to the incubator for 2-3 min. After 2-3 min, check for dislodged cells under microscope and add 8 mL of RPMI to deactivate trypsin.
7. Collect the cell suspension in a 15 mL conical tube and centrifuge at 314 x g for 5 min to get a pellet. Discard the supernatant. Wash the cell pellet with 1 mL of 1x PBS, suspend the pellet in 5 mL of RPMI and determine the cell density using a hemacytometer[15]. Centrifuge yhe remaining cell solution at 314 x g for 5 min to obtain a pellet.
8. Suspend the pellet in RPMI to obtain a concentration of 4 x 10^5 cells/10 µL. Take 5 µL of the cell suspension and 5 µL of matrigel to make 10 µL of cell solution for each injection.

4. Ultrasound Guided Adrenal Gland (NB) or Renal Sub Capsule (ES) Implantation

NOTE: All ultrasound procedures are performed using a high resolution *in vivo* imaging system. For the described procedures, the transducer, which has a center frequency of 40 MHz and a bandwidth of 22-55 MHz was used.

1. Utilize 6-8-week-old immune-deficient NSG mice for all injection procedures.
2. Chill the matrigel and autoclaved Hamilton syringes fitted with a 27G needle (1.25"), and 22G catheters (0.9 mm external diameter, 25 mm length) overnight at 4 °C.
3. Place the cell solution prepared in step 3 on ice.
4. Anesthetize the mice in an induction chamber using 2% isoflurane in O_2 delivered at 2 L/min.
   NOTE: Adequate anesthesia is determined with the lack of active movement and the maintenance of spontaneous respiration.
5. Once anesthetized, depilate the back and flank of the animals using hair removal lotion (such as Nair) and a shaver.
6. Transfer the animal to the imaging platform with abdominal side down, where the nose of the animal is placed into a nosecone and secured while inhaling isoflurane.
7. Place optical ointment in the animal's eyes to prevent drying. Tape the mouse in place to prevent any inadvertent movement.
8. Identify the murine liver, vena cava, spleen, left kidney, and adjacent left adrenal gland using ultrasound visualization.
9. Use sterile gloves, mask and cap for personal protection and maintenance of sterile conditions. Under ultrasound-guidance, gently insert a 22G catheter through the skin and back muscle directly into the left adrenal gland to provide a channel for cellular injection. Remove the needle and leave the catheter in place.
10. Load a chilled Hamilton syringe fitted with a small-bore needle with 10 µL of cell solution, then guide the syringe stereotactically through the catheter positioned into the center of the adrenal gland.
11. Inject the cells into the targeted adrenal tissue. Leave the needle in place for 1-2 min to allow the matrigel to set. Slowly remove the needle, followed by the removal of the catheter.
12. Place the mice back into their cage and ensure that the mouse regains sufficient consciousness to maintain sternal recumbency.
    NOTE: Due to the minimally invasive nature of this technique, post procedural pain is minimal, but still monitored on a daily basis with mice health checks." should be followed with a sentence: "If unexpected signs of pain or distress are identified during the course of an experiment, consult with your institutional veterinary support unit for information regarding analgesia or other medical care.

Representative Results

Using the procedures presented, ultrasound-guided implantation of NB cells into the adrenal gland was done in a dedicated procedure room equipped with a heated surgical table. Arm and foot pads were placed for monitoring murine heart activity (**Figure 1A**). The animal remained anesthetized under isoflurane using nose cone inhalation. Using a high-resolution ultrasound probe, the left kidney was identified with the adrenal gland just cranial to the kidney (**Figure 1B**). The needle was then advanced into the adrenal gland under direct visualization (**Figure 1C**). During initial utilization of this technique, a mixture of methylene blue dye and matrigel was used to confirm correct localization of the adrenal gland. The animal was sacrificed, and the success of the procedure was confirmed on necropsy by visualizing methylene blue dye beneath the adrenal gland capsule (**Figure 1D**).

Weekly ultrasound and bioluminescence imaging were the modalities used to monitor tumor engraftment and growth rate. Bioluminescence imaging of the region of interest was measured as photons/s/cm^2/steridian (p/s/cm^2/sr) with a minimal count of 10^6 to 10^8 indicative of adequate tumor size for preclinical experiments[9] (**Figure 2**). Analysis using *t*-test showed statistically significant increase in bioluminescence was noted over the eight-week period (*p<0.05; **p<0.001; ***p<0.0001). Ultrasound imaging allowed noninvasive measurements of tumor area and volume. This along with bioluminescence measurement monitored both tumor engraftment and progression (**Figure 3**). Similar procedures were utilized for ES cells injected into the renal sub capsule (**Figure 4**).

Gross and histological analysis of resultant tumors characterized the primary tumors and metastases at necropsy. Tissue samples were examined for morphologic cell patterns and stained for tumor-specific protein markers (**Figure 5**, **Figure 6**). Primary tumor engraftment for NB cell lines (IMR32, SH-SY-5Y, SK-N-BE2, UMNBL001, UMNBL002) ranged from 62-100%, with metastases seen in 0-100% of injected mice. The most robust metastases were seen in the SK-N-BE2 (33%) and UMNBL002 (100%). Metastatic sites for NB were lymph nodes, liver, lung and cortical bone. Renal sub capsular engraftment for ES cell lines (A4573, A673, CHLA-25, TC-32) ranged from 60-100%, with metastases seen in 0-40% of injected mice. Metastatic sites examined for ES included lymph nodes, cortical bones and lungs. The most robust engraftment (100%) and metastases (40%) were seen in TC-32 xenograft mice.

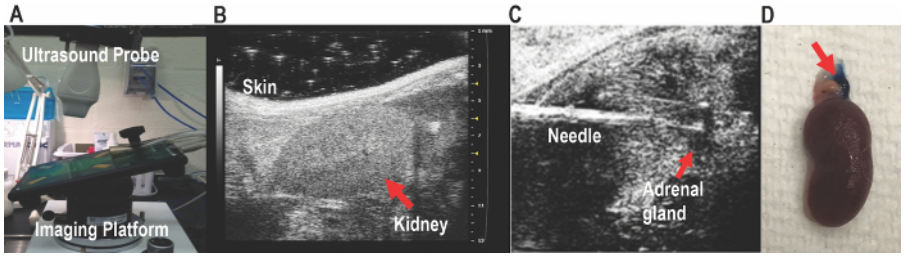

Figure 1. Murine adrenal gland localization and ultrasound-guided NB cell implantation. (A) High resolution ultrasound imaging of murine abdominal organs allowed adrenal gland implantation of tumor cells. (B) Left kidney was identified. (C) The left adrenal gland is located adjacent to the left kidney as a hypoechoic (dark) round structure. The needle was advanced into the adrenal gland followed by cell injection. (D) A mixture of matrigel and methylene blue dye was used to assess the accuracy of injection procedures. Representative *ex vivo* image of the left kidney and adrenal gland with matrigel and methylene blue dye at the adrenal gland capsule and peri-adrenal space. This figure has been modified with permission from Van Noord, R.A. *et al*.[11]. Please click here to view a larger version of this figure.

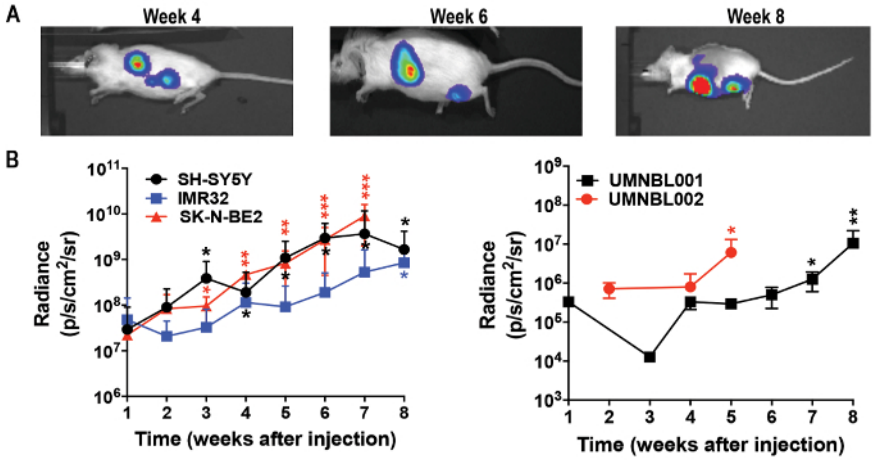

Figure 2. *In vivo* bioluminescence imaging of tumor engraftment and growth rate. (A) Human NB adrenal xenografts were monitored for engraftment and tumor growth over eight weeks. (B) Maximal bioluminescence signal was determined within the region of interest. NB cell lines (SH-SY5Y, IMR 32, SK-N-BE2) and patient-derived cells (UMNBL001, UMNBL002) had increased radiance and growth patterns over time. Increase of bioluminescence over the eight-week period was statistically significant (*p<0.05; **p<0.001; ***p<0.0001). This figure has been modified with permission from Van Noord, R.A. *et al*.[11]. Please click here to view a larger version of this figure.

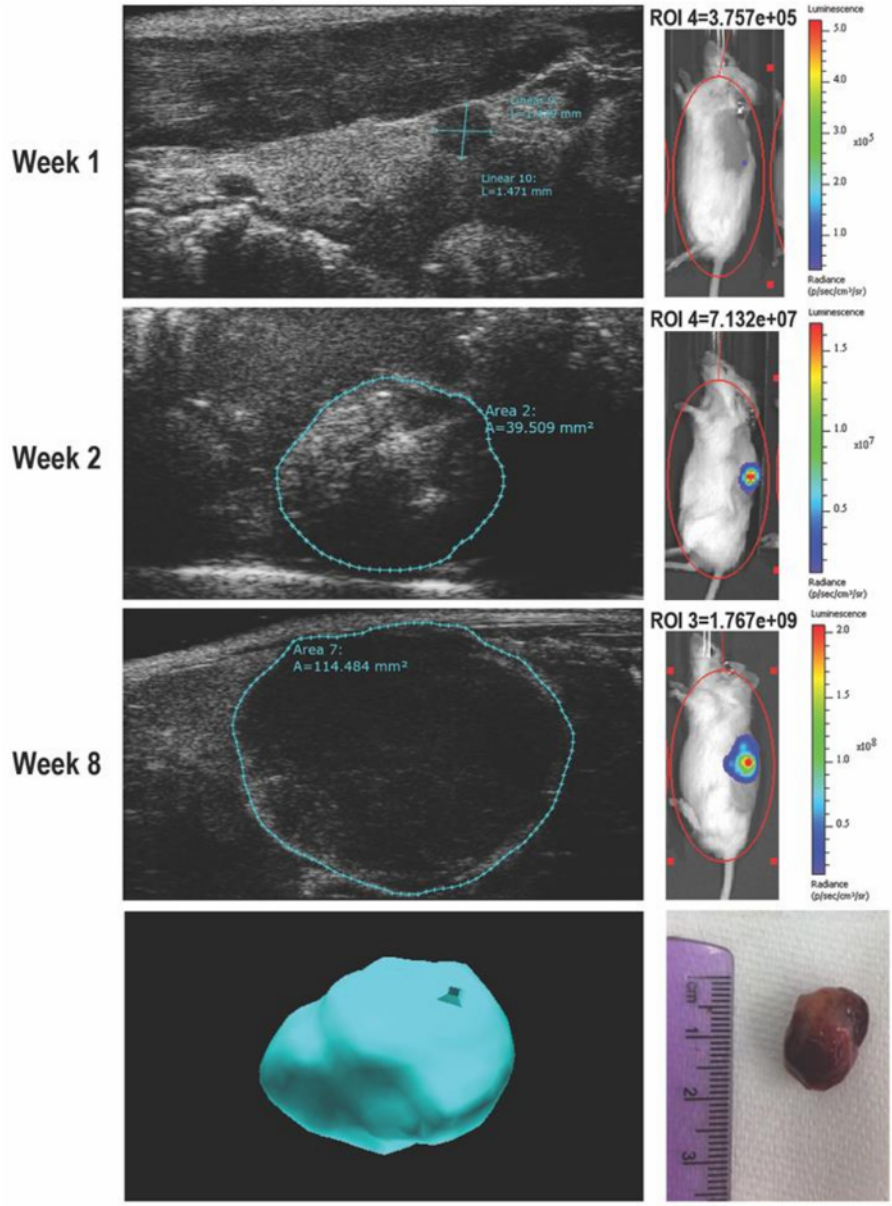

Figure 3. *In vivo* ultrasound imaging of tumor engraftment and growth. Ultrasound imaging monitored *in vivo* tumor progression. Ultrasound images and corresponding bioluminescence images at one, two and eight weeks are shown. At one week, engraftment was visualized in both imaging modalities. Tumor area and volume were calculated using ultrasound imaging. 3D ultrasound images mirrored excised tumors at the completion of the study. This figure has been modified with permission from Van Noord, R.A. *et al.*[11]. Please click here to view a larger version of this figure.

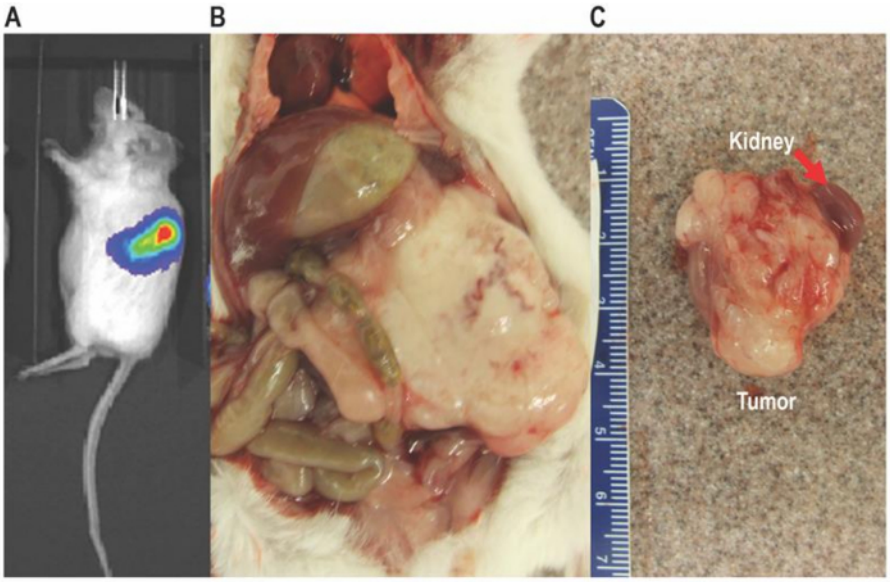

Figure 4. Murine kidney localization and ultrasound-guided implantation of ES cells. (A) Bioluminescence was used to monitor tumor radiance and growth. (B-C) Animals developed locally invasive tumors that distorted surrounding abdominal structures and invaded into local structures such as muscle. This figure has been modified with permission from Van Noord, R.A. *et al.*[11]. Please click here to view a larger version of this figure.

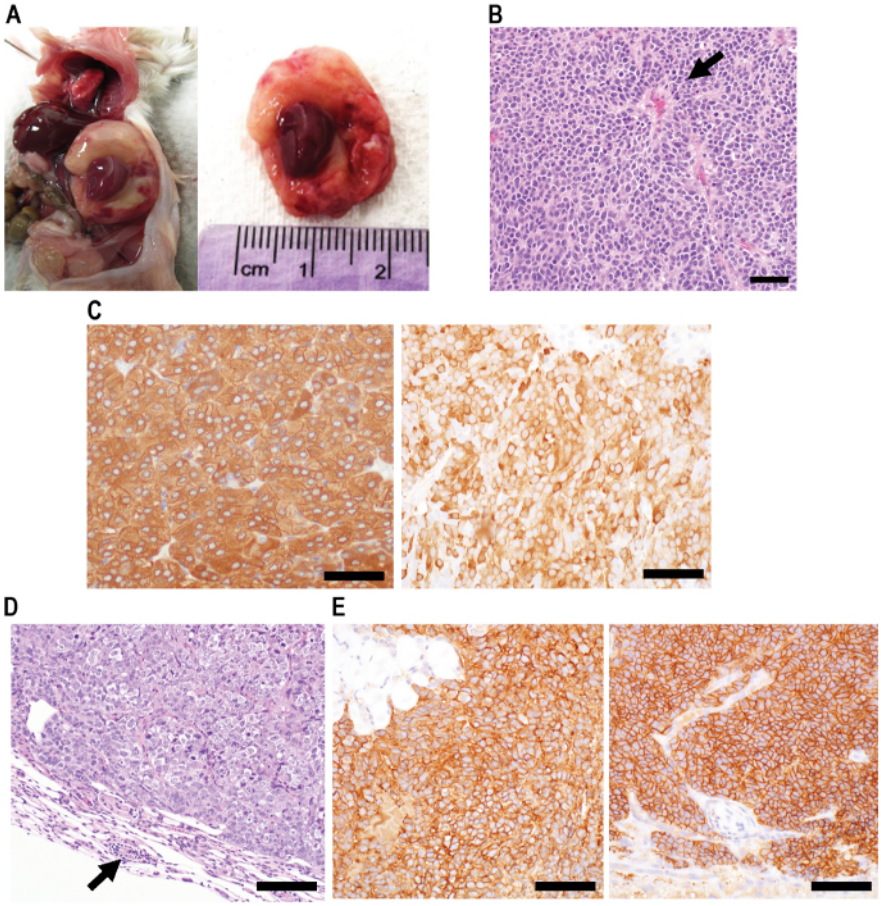

Figure 5. Tumor histopathology of NB and ES xenograft tumors. (A) NB xenograft mice had locally infiltrative primary tumors at the adrenal and peri-adrenal gland sites, which distorted adjacent abdominal organs. (B) Microscopically (20X, bar = 50 µm), the xenograft adrenal tumors showed morphologic features consistent with human NB (clusters of poorly differentiated angular to round cells), including occasional pseudo rosette formation (arrow). (C) Tumor tissue showed strong tyrosine hydroxylase (NB tumor marker) immunoreactivity (40X, bar = 40 µm; positive control staining shown in the left panel; 1:100). (D) ES xenograft tumor had histologic features consistent with infiltrative ES (40X, bar = 40 µm), clusters of angular to round epithelioid cells separated by a fine fibro vascular stroma, effacing and compressing normal adjacent kidney (arrow; compressed remnants of kidney parenchyma). (E) ES tumor tissue showed strong membrane immunoreactivity for the ES tumor marker CD99 (40X, bar = 40 µm; positive control staining shown in the left panel; 1:100). This figure has been modified with permission from Van Noord, R.A. *et al.*[11]. Please click here to view a larger version of this figure.

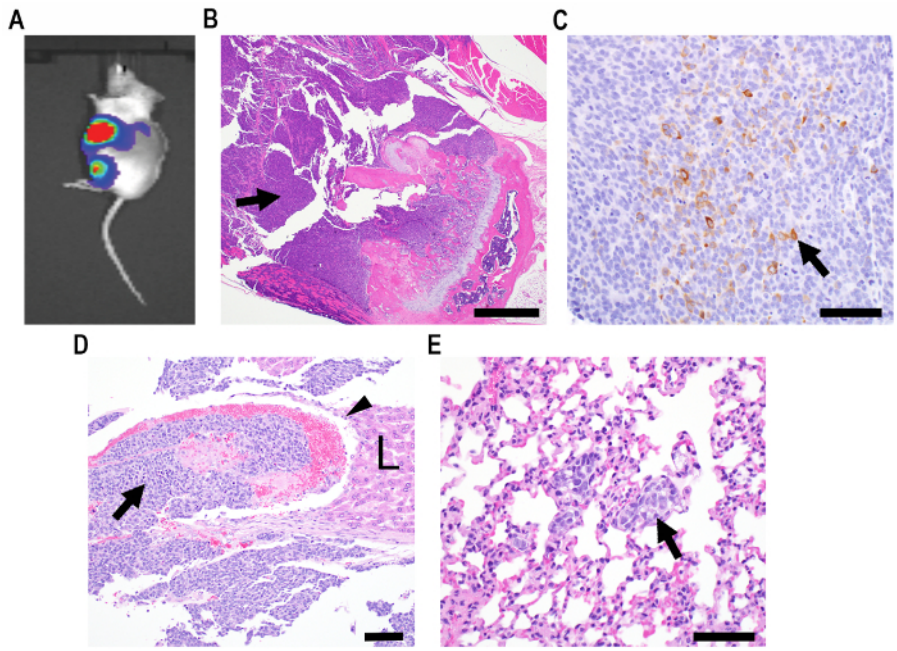

Figure 6. Distant metastases developed in xenografts established by ultrasound-guided injection technique. (A) Bioluminescence imaging showing the primary NB tumor at the adrenal gland space and metastatic foci detected at cortical bone. (B) Microscopic analysis demonstrated a metastatic tumor (arrow) effacing the marrow cavity and cortical bone of the proximal femur (4X, bar = 400 µm). (C) Tyrosine hydroxylase cytoplasmic immunoreactivity of the cortical bone NB metastatic site (40X, bar = 40 µm). (D) Microscopy of patient-derived orthotopic xenograft (UMNBL002) with a hepatic metastasis (arrow) within a hepatic vein (arrowhead demonstrates endothelial cells), and infiltrating the adjacent liver (L) parenchyma (20X, bar = 50 µm). (E) Neuroblastoma micro metastasis (arrow) within the lung parenchyma (40X, bar = 40 µm). This figure has been modified with permission from Van Noord, R.A. *et al.*[11]. Please click here to view a larger version of this figure.

Discussion

Ultrasound-guided implantation of NB and ES cells is an efficient and safe method to establish reliable murine xenografts for preclinical studies in cancer biology. Critical to the success of ultrasound-guided tissue-targeted implantation is the presence and availability of trained personnel with expertise in anatomically localizing the organ of interest and in stereotactic injection of tumor cells.

The dissociation of tumor tissue proved to be a crucial step in developing the described patient-derived xenograft model. Native tumor tissue includes a cellular microenvironment and surrounding stroma that may affect the tumor uptake or engraftment. Cell counts, after the dissociation process was complete, provided a gauge of the cellular density in the sample, with 2 x 10^5 cells/10 µL considered an optimal cell count for implantation and successful tumor engraftment.

Luciferase tagging of cells allowed for the validation of tumor engraftment and monitoring of tumor growth by measuring bioluminescence signal, with 10^6 to 10^8 being considered indicative of tumor uptake[9]. To ensure successful transduction, luciferase activity was confirmed *in vitro* prior to injection of cells. This was done by immunofluorescence, luciferase assay kits, and also by examining the cells for bioluminescence signal. Settings used to measure bioluminescence were kept constant, providing consistent data during weekly measurements.

Ex vivo histopathological analysis of tumors confirmed the cell type and morphology of resultant tumors with specific staining for protein markers. Histopathological analysis confirmed tumor engraftment and metastasis demonstrated by ultrasound and bioluminescent imaging.

Advantages of ultrasound-guided cellular implantation include its non-invasive nature, minimal animal recovery time, and growing success in the establishment of several successful xenograft models. Ultrasound imaging also provides a reliable method to monitor *in vivo* tumor progression and tumor volumes. In these preclinical models, tumors progressed to locally invasive disease with metastasis within 5 weeks. Limitations include the availability of high resolution imaging technology and the ability to consistently localize the target organ. Availability of personnel with expertise in ultrasound imaging of the organ of interest are critical components of this technique.

The availability of high-resolution ultrasound imaging has increased substantially within the last decade and its use continues to expand not only in the clinical practice but also in laboratory research. The utilization of ultrasound for the development of modern murine xenografts is a promising application, with potential for advancing preclinical research models for cancer drug discovery.

Disclosures

The authors have no disclosures.

Acknowledgements

This work received support from the Robert Wood Johnson Foundation/Amos Medical Faculty Development Program, Taubman Research Institute, and the Section of Pediatric Surgery, The University of Michigan. The authors wish to thank Kimber Converso-Baran and Dr. Marcus Jarboe for the assistance with ultrasound injection procedures and the imaging platform. We thank Paul Trombley for his assistance with figure graphics. We also thank the Department of Radiology at The University of Michigan for the use of The Center for Molecular Imaging and the Tumor Imaging Core, which are supported in part by Comprehensive Cancer Center NIH, grant P30 CA046592. The University of Michigan Physiology Phenotyping Core that is supported in part by grant funding from the NIH (OD016502) and the Frankel Cardiovascular Center. Cell line authentication was done at IDEXX RADIL Bioresearch Facilities, Columbia, MO. We thank Tammy Stoll, Dr. Rajen Mody and the Mott Solid Tumor Oncology Program. Our patients and families are gratefully acknowledged for their inspiration, courage, and ongoing support of our research.

References

1. Sanmamed, M.F., Chester, C., Melero, I., Kohrt, H. Defining the optimal murine models to investigate immune checkpoint blockers and their combination with other immunotherapies. *Ann Oncol.* **27** (7) 1190-1198 (2016).
2. Fidler, I.J., Hart, I.R. Biological diversity in metastatic neoplasms: origins and implications. *Science.* **217** (4564) 998-1003 (1982).
3. Bibby, M.C. Orthotopic models of cancer for preclinical drug evaluation. *Eur J Cancer.* **40** (6) 852-857 (2004).
4. Killion, J.J., Radinsky, R., Fidler, I.J. Orthotopic Models are Necessary to Predict Therapy of Transplantable Tumors in Mice. *Cancer Metastasis Rev.* **17** (3) 279-284 (1998).
5. Daniel, V.C. *et al.* A primary xenograft model of small-cell lung cancer reveals irreversible changes in gene expression imposed by culture in vitro. *Cancer Res.* **69** (8) 3364-3373 (2009).
6. Khanna, C., Jaboin, J.J., Drakos, E., Tsokos, M., Thiele, C.J. Biologically relevant orthotopic neuroblastoma xenograft models: Primary adrenal tumor growth and spontaneous distant metastasis. *In Vivo.* **16** (2) 77-85: (2002).
7. Stewart, E. *et al.* Development and characterization of a human orthotopic neuroblastoma xenograft. *Dev Biol.* **407** 344-355 (2015).
8. Jäger, W. *et al.* Minimally Invasive Establishment of Murine Orthotopic Bladder Xenografts. *J. Vis. Exp.* (84), e51123 (2014).
9. Teitz, T. *et al.* Preclinical Models for Neuroblastoma: Establishing a Baseline for Treatment. *PLoS ONE.* **6** (4) e19133 (2011).
10. Braekeveldt, N. *et al.* Neuroblastoma patient-derived orthotopic xenografts retain metastatic patterns and geno- and phenotypes of patient tumours. *International Journal of Cancer.* **136** (5) 252-261 (2015).
11. Van Noord, R.A. *et al.* Tissue-directed Implantation Using Ultrasound Visualization for Development of Biologically Relevant Metastatic Tumor Xenografts. *In Vivo.* **31** (5) 779-791 (2017).
12. Vormoor, B. *et al.* Development of a Preclinical Orthotopic Xenograft Model of Ewing Sarcoma and Other Human Malignant Bone Disease Using Advanced In Vivo Imaging. *PLoS ONE.* **9** (1) e85128 (2014).
13. Hakky, T. S., Gonzalvo A. A., Lockhart, J. L., Rodriguez, A. R. Primary Ewing sarcoma of the kidney: a symptomatic presentation and review of the literature. *Ther Adv Urol.* **5** (3) 153-159 (2013).
14. Cheng, H., Clarkson, P.W., Gao, D., Pacheco, M., Wang, Y., and Nielsen, T.O. Therapeutic Antibodies Targeting CSF1 Impede Macrophage Recruitment in a Xenograft Model of Tenosynovial Giant Cell Tumor. *Sarcoma.* **2010.** 174528-7, (2010).
15. JoVE Science Education Database. *Basic Methods in Cellular and Molecular Biology.* Using a Hemacytometer to Count Cells. JoVE, Cambridge, MA, (2018).

